Correspondence to:
S. Komiya,
skomiya@bgc-jena.mpg.de

Stable Carbon Isotope Studies of CH_4 Dynamics Via Water and Plant Pathways in a Tropical Thai Paddy: Insights Into Diel CH_4 Transportation

Shujiro Komiya[1] , Tomotsugu Yazaki[2] , Fumiyoshi Kondo[3], Kentaro Katano[4,5], Jost V. Lavric[1] , Iain McTaggart[2], Tiwa Pakoktom[6], Meechai Siangliw[7], Theerayut Toojinda[7], and Kosuke Noborio[2]

[1]Max Planck Institute for Biogeochemistry, Jena, Germany, [2]School of Agriculture, Meiji University, Kawasaki, Japan, [3]Japan Coast Guard Academy, Kure, Japan, [4]Graduate School of Agriculture, Meiji University, Kawasaki, Japan, [5]Now at Japan International Cooperation Agency, Tokyo, Japan, [6]Department of Agronomy, Faculty of Agriculture at Kamphaeng Saen, Kasetsart University, Nakhon Pathom, Thailand, [7]National Center for Genetic Engineering and Biotechnology, Khlong Luang, Pathum Thani, Thailand

Abstract Separate evaluation of methane (CH_4) emission dynamics (e.g., oxidation, production, and transportation) at the soil-plant-atmosphere and soil-water-atmosphere interfaces has been limited in tropical rice paddies, but it is crucial for comprehending the entire CH_4 cycles. We investigated CH_4 oxidation, production, and transportation through plant and water pathways during the reproductive stage in a tropical Thailand rice paddy field using natural abundance carbon stable isotope ratios ($\delta^{13}CH_4$ and $\delta^{13}CO_2$). Mass balance equations using $\delta^{13}CH_4$ and $\delta^{13}CO_2$ in soil gases indicated that CH_4 oxidation in the planted soil exceeded those in the interrow soil due to oxygen supply through rice roots. In addition, at 1–11 cm depth acetate fermentation was the dominant process in the planted soil, whereas in the interrow soil the dominant process was H_2/CO_2 reduction. The water pathway showed a significant negative correlation between CH_4 flux and released $\delta^{13}CH_4$ over 24 hr, driven by a diel change in episodic ebullition, steady ebullition, and diffusion, all due to diel changes in soil temperature and atmospheric pressure. In contrast, the plant pathway showed a significant positive relationship between CH_4 flux and emitted $\delta^{13}CH_4$ throughout one day. A comparison of the diel change in emitted $\delta^{13}CH_4$ between the water and plant pathways showed that the rice plants transported CH_4 in soil bubbles without any large isotopic fractionation. The diel change in the plant-mediated CH_4 transportation was mainly controlled by diel changes in soil bubble expansion and CH_4 diffusion through plants, which were probably regulated by diel changes in soil temperature and atmospheric pressure.

Plain Language Summary Methane (CH_4) emissions from paddy soil are mainly controlled by three processes: CH_4 production, CH_4 oxidation (consumption), and CH_4 transportation from soil to plant, water, and ultimately the atmosphere. There are two emission pathways, the soil-plant-atmosphere and soil-water-atmosphere interfaces, but there has not been much detailed evaluation of the different characteristics of the three processes in the two pathways. Here we evaluated CH_4 production, oxidation, and transportation at the soil-plant-atmosphere and soil-water-atmosphere interfaces during the reproductive stage of rice in a tropical Thailand paddy field. We found that in planted soil there was more CH_4 production by acetate fermentation and more CH_4 oxidation, due to more organic matter and oxygen supply, respectively, through plant roots. Methane was transported through water by three modes: episodic bubble ebullition, steady bubble ebullition, and diffusion. Diel variation in the rates of these three transportation modes was related to diel changes in soil temperature and atmospheric pressure. Methane in soil bubbles was also transported into the atmosphere through rice plants. Diel variation in the CH_4 transportation through rice plants was related to diel change in bubble expansion, which was also mainly regulated by diel changes in soil temperature and atmospheric pressure.

1. Introduction

Increasing concentration of atmospheric methane (CH_4) contributes to global climate change (Bindoff et al., 2013). CH_4 emissions from anthropogenic sources account for 54–72% of the total global

CH$_4$ emission, and rice paddy fields are one of the largest anthropogenic CH$_4$ sources (Bridgham et al., 2013). The estimated CH$_4$ emission from global rice paddies ranges between 23 and 40 Tg CH$_4$ year^{-1} (Saunois et al., 2016), so there is still large uncertainty. Yan et al. (2009) reported that 90% of CH$_4$ emission from rice paddies is derived from tropical Asia. So, in order to reduce the uncertainty, further field observations and better comprehension of CH$_4$ emission dynamics in tropical rice paddies are needed.

During irrigated rice cropping seasons, CH$_4$ is mainly produced from fermentation of acetate and reduction of carbon dioxide with hydrogen (H$_2$/CO$_2$) by methanogens under anaerobic conditions in the submerged soil (Conrad, 2005; Takai, 1970; Whiticar et al., 1986). Some of the soil CH$_4$ is oxidized by methanotrophic bacteria in the aerobic surface soil and rice rhizosphere soil where sufficient oxygen is supplied from the atmosphere through the rice aerenchyma system (Schütz et al., 1989). In paddy soil, the release of CH$_4$ into the atmosphere is mainly through rice plants, and via bubble ebullition, categorized into episodic ebullition and steady ebullition, or diffusion through paddy water, including hydrodynamic transport that mainly comprises of molecular diffusion and advection processes (Chanton, 2005; Coulthard et al., 2009; Green, 2013; Poindexter et al., 2016; Schütz et al., 1989).

The CH$_4$ emission dynamics in rice paddies are mainly controlled by CH$_4$ production, oxidation, and transportation processes (Schütz et al., 1989). Plant-mediated transportation usually dominates overall CH$_4$ emission (90%) (Butterbach-Bahl et al., 1997; Schütz et al., 1989), so studies of CH$_4$ emission dynamics often do not pay enough attention to evaluating separately the plant- and water-mediated pathways (Chanton et al., 1997; Khalil et al., 2008; Marik et al., 2002; Miyata et al., 2005; Rao et al., 2008; Tyler et al., 1994; Yagi et al., 1994; Zhang et al., 2011, 2012, 2017). For example, a study showed that CH$_4$ ebullition through paddy water accounted for 35–62% of total CH$_4$ emissions when rice straw was applied to tropical rice paddy fields (Wassmann et al., 1996). The organic matter (e.g., rice straw, root exudates, and decayed root) supply stimulates production of CH$_4$ that generally exists in the gas-phase (i.e., soil bubbles) rather than the liquid-phase (i.e., soil solution) due to low CH$_4$ solubility; eventually this increases CH$_4$ ebullition through paddy water (Hayashi et al., 2015; Schütz et al., 1989; Tokida et al., 2013; Wassmann et al., 1996). Therefore, the potential for such large water-mediated CH$_4$ emission makes it difficult to accurately understand the true nature of CH$_4$ emission dynamics in rice paddy fields. Thus, the plant-mediated pathway needs to be assessed separately from the water-mediated pathway and vice versa. Separate investigation of CH$_4$ emission dynamics via plant- and water-mediated pathway is limited, but it is essential to properly understand the entire CH$_4$ dynamics (Bridgham et al., 2013).

Natural abundance stable carbon isotope methods are useful for understanding the main controlling processes of CH$_4$ emission dynamics in rice paddy fields: CH$_4$ production, oxidation, and transportation (Chanton, 2005; Conrad, 2005; Tyler et al., 1997). The different δ^{13}C values of CH$_4$, CO$_2$, and acetate make it possible to estimate the relative contribution of acetate- and H$_2$/CO$_2$-dependent methanogenesis to total CH$_4$ production, and the proportion of CH$_4$ consumption by methanotrophs (Conrad, 2005; Krüger et al., 2002; Tyler et al., 1997). Additionally, differences in δ^{13}C of emitted CH$_4$ between the plant-mediated pathway, bubble ebullition, and diffusion via paddy water would enable evaluation of the CH$_4$ transportation modes from paddy soil to the atmosphere (Chanton, 2005; Tokida et al., 2014). Therefore, the application of the natural abundance stable carbon isotope methods to plant- and water-mediated pathways individually should help to clarify the contributions of these three main processes to CH$_4$ emissions via each pathway.

To date, most δ^{13}CH$_4$ studies in rice paddy fields have investigated seasonal variations in CH$_4$ production, oxidation, and transportation processes (Bilek et al., 1999; Krüger et al., 2002; Marik et al., 2002; Nakagawa et al., 2002; Tyler et al., 1994, 1997; Zhang et al., 2011, 2012, 2013, 2016, 2017), but few have focused on diel variations. Two studies that have focused on diel variations of δ^{13}CH$_4$ showed that δ^{13}CH$_4$ emitted from rice paddies positively correlated with increasing CH$_4$ flux due to increasing transpiration rate or bubble ebullition (Chanton et al., 1997; Marik et al., 2002). However, both these studies only measured δ^{13}CH$_4$ emitted through the mixed (both plant- and water-mediated) pathways using chambers; that is, the chambers measured not only the plant-mediated CH$_4$ transportation but also water-mediated transport. Thus, the diel variations in the two pathways remain unclear.

In this study, we applied natural carbon stable isotope methods to soil gas measurement in interrow and planted soils and to automatic plant and water chamber measurements. By using the isotopic measurements, we evaluated CH_4 emission dynamics (i.e., CH_4 oxidation, production, and transportation) at the respective soil-plant-atmosphere and soil-water-atmosphere interfaces during the reproductive stage in a tropical rice paddy in Thailand, one of the largest rice producing countries in tropical Asia (FAOSTAT, 2018). In particular, we examined the differences in soil CH_4 oxidation and production (e.g., acetate fermentation and H_2/CO_2 reduction) between interrow and planted soils. We used soil and emitted $\delta^{13}CH_4$ values to assess the soil depths at which the methane that was transported into the atmosphere through the respective water and plant pathways originated. Also, using the soil and chamber measurements we attempted to partition the water-mediated CH_4 transportation into bubble ebullition (episodic and steady) and diffusion, as well as examining diel CH_4 transportation through the respective water and plant pathways. The specific research questions are summarized below:

1. What are the differences in CH_4 oxidation and CH_4 production (i.e., acetate fermentation and H_2/CO_2 reduction) processes between planted and interrow soils?
2. At which soil depths did the soil CH_4 transported into the atmosphere through the water and plant pathways originate?
3. What is the diel variation in CH_4 transportation through the water (e.g., episodic bubble ebullition, steady bubble ebullition, and diffusion) and plant pathways, and how is it regulated?

2. Materials and Methods

2.1. Study Site and Measurement Period

Field experiments were carried out between 13 September and 28 September (DOY: 256–271) in 2014 in a farmer's rice paddy field at Kasetsart University (14°00′33″N, 99°59′03″E), Kamphaeng Saen campus in Nakhon Pathom Province, Thailand. The paddy soil was classified as clay soil (65.7% clay; 23.30% silt; 11.0% sand) with a dry bulk density of 1.69 Mg m^{-3}. The topsoil, sampled on DOY 260, had a soil pH of 5.98 (1:1, soil:water). Weeds and weedy rice were directly plowed into the paddy field soil on DOY 168 and 177, and then on DOY 181, seedlings of the rice variety "Homcholasit" were transplanted to the field with four to five seedlings planted in each location, 18 cm apart in the same row, with rows 30 cm apart. The heading of the rice plants began on DOY 265. The soil was continuously flooded from DOY 168 to 301 (harvest day) with the water depth ranging between 2–20 cm. During the gas measurement period, the flooding water depth was as follows. From the start of the gas measurements on DOY 256 until 10:50 a.m. local time (LT) on DOY 267, the water depth fell from 7.8 to 2.5 cm (Figure S1g in the supporting information). Then, after irrigation at 10:50 a.m. LT on DOY 267 and heavy rain on the same day (21.9 mm day^{-1}), the water depth rose to 10.6 cm by 12:35 a.m. LT on DOY 268. Thereafter, it declined again to 6.9 cm by 5 p.m. LT on DOY 271 (Figure S1g).

2.2. Soil Gas Sampling and Measurement

The gases in the paddy soil and water were collected using diffusive equilibration samplers. The diffusive equilibration samplers consisted of a PVC pipe (id = 38 mm, od = 39 mm, and length = 400 mm) with several drilled holes of 7 mm dia. and a 0.5 mm thick silicon sheet which entirely covered the pipe (Figure S2), similar to Kato et al. (2013). The side of the silicon sheet in contact with the soil/water was protected by wrapping that side of the sheet in a plastic mesh. Both ends of the sampler were sealed with silicone rubber stoppers, and one of the rubber stoppers was connected to a nylon tube which was extended above ground in order to collect the gas samples from the samplers. On DOY 211, the soil gas samplers were buried horizontally at 1–5, 7–11, and 13–17 cm depths under both a rice hill and an interrow space between rice plants (Figure S3). On the same day, the water gas sampler was submerged flat in the paddy water. Gas samples were taken from under the planted soil by plastic syringes at noon LT on DOY 257, 260, 261, 263, and 269. The gases in the interrow soil and surface water were collected at noon LT on DOY 257, 260, 263, and 269. After each sampling of the water or soil gases, atmospheric air was drawn into the samplers automatically due to negative pressure inside the samplers themselves. Then, the above ground end of the nylon tube was sealed by a three-way stopcock to prevent gas exchange between the sampler and atmosphere during nonmeasurement periods. Since the samplers needed to equilibrate with surrounding gases for 11 hr, a gas sampling interval of at least 1 day was assumed to be enough for gas equilibration between air inside the samplers and the

soil/water gases. We measured the concentration and $\delta^{13}C$ of CH_4, CO_2 in the soil/water gas samples, which were diluted 81× or 101× with high-purity nitrogen gas, using a wavelength-scanned cavity ring-down spectroscopy (WS-CRDS) analyzer (G2201-i, Picarro Inc., Santa Clara, CA, USA). In the laboratory test, we found an isotopic fractionation across the diffusive equilibration sampler for CH_4: +1.8‰ (unfortunately not assessed for CO_2). The isotopic fractionation was subtracted from the $\delta^{13}CH_4$ measured by the samplers. This isotopic fractionation was also subtracted from the $\delta^{13}CO_2$ values measured by the samplers with the assumption that the isotopic fraction for CH_4 was as same as that for CO_2.

2.2.1. Calibration

The $\delta^{13}CH_4$ measurement was calibrated using two CH_4 working standard gases: $\delta^{13}CH_4 = -43.3‰$ (999 ppm CH_4, 1,000 ppm CO_2, N_2 balance, VPDB) and $\delta^{13}CH_4 = -66‰$ (1,000 ppm CH_4, N_2 balance, VPDB) in a laboratory after the field observation (Table S1). Additionally, the CH_4 working standard gas (999 ppm CH_4, $\delta^{13}CH_4 = -43.3‰$) was diluted to two CH_4 concentration levels, 6.0 and 14 ppm, by using high-purity nitrogen gas. This dilution test demonstrated that $\delta^{13}CH_4$ measurements by the WS-CRDS analyzer were not affected by CH_4 concentration (Table S1). The $\delta^{13}CO_2$ measured by the WS-CRDS analyzer was also calibrated by two CO_2 working standard gases: $\delta^{13}CO_2 = -9.47 \pm 0.04‰$ (403 ppm CO_2, N_2/O_2 balance, VPDB) and $\delta^{13}CO_2 = -34.73 \pm 0.03‰$ (9,790 ppm CO_2, N_2 balance, VPDB) (Table S1). Before the calibration, the high CO_2 gas concentration (9,790 ppm) was diluted to 3400.14 ppm with high-purity nitrogen gas because the original concentration was too high for the WS-CRDS analyzer.

2.3. Automatic Plant and Water Chamber Measurements

The emissions of CH_4 and $\delta^{13}CH_4$ through rice plants and paddy water were measured using two polycarbonate automated closed chambers (Green Blue Corp., Tokyo, Japan; Figure S3). On DOY 232 (20 August), one of the chambers (24 × 24 cm at the base and 140 cm tall) was placed over a rice hill with the lid left open. Starting on DOY 256, the water surface at the bottom of the plant chamber was covered by air bubble cushioning wrap, with assumed minimal gas permeability, to prevent methane emissions via paddy water, so that (as much as possible) the chamber only captured CH_4 transported through the rice plants. It is still possible that some water-mediated CH_4 emission could be captured in the chamber due to transported along the hydrophobic rice plant exterior. However, the uncovered water-surface area exposed to the atmosphere was very small, only a very small area between the plant culms, so we believe that this chamber, the plant chamber, predominantly measured CH_4 emitted through the plant pathway. The other chamber (50 × 20 cm at the base and 40 cm height) was inserted between rice plants on DOY 220 to measure the CH_4 exchanges via paddy water. From DOY 256 to 271, the top lids of both chambers were automatically closed for 10 min every hour, to measure the CH_4 fluxes and emitted $\delta^{13}CH_4$. The headspace air in each chamber was mixed during lid closure using a small electric fan which was incorporated into each chamber. The fan in the plant chamber also ran during nonmeasurement periods when the lids were open in order to prevent gas residence at the bottom of the tall chambers. During the lid closure period, the headspace air in each chamber was circulated through a 250 ml buffer tank, placed inside a shed about 4 m from each chamber, at 500 ml min^{-1} flow rate by a diaphragm pump (TD-4X2N, Brailsford Co., Rye, NY, USA). Another diaphragm pump (UN84.4 ANDC-B, KNF Neuberger Inc., NJ, USA; flow rate ~25 ml min^{-1}) sucked the headspace air in the buffer tank through the WS-CRDS analyzer, calibrated as described in section 2.2.1, which monitored the change in CH_4 concentration and $\delta^{13}CH_4$ in each chamber at around 3.6 s intervals in the high precision (HP) and high dynamic range (HR) modes. In case of an abrupt CH_4 concentration increase for a short period time, measurement artifacts occurred in the HR mode data stream and afterwards the measurement returned to normal. No such artifacts occurred in the HP mode, but the HP mode could only measure CH_4 concentrations up to 15 ppm. So only the HR mode continuously measured CH_4 concentration and $\delta^{13}CH_4$, including times when the CH_4 concentration exceeded 15 ppm. The analyzed air was returned to the loop line, but before the sampled air entered the analyzer, the air was dehumidified by a membrane dryer (SWG-A01-06, Asahi Glass Engineering Co., Chiba, Japan) to water vapor concentration of less than 0.1%. The initial air after closing the chambers reached the WS-CRDS analyzer in about 2 min, estimated from the internal volumes of the buffer tank and connecting tubes and also the flow rate of the two pumps. Each chamber measurement was finished when the lid of the chamber opened, so that one measurement cycle for each chamber ran for 8 min. The respective plant and water chamber measurements were conducted every hour at 32 and 50 min after the hour.

The methane flux was calculated using an exponential method (de Mello & Hines, 1994) following Komiya et al. (2015) (Figure S4a). In cases when the exponential method did not fit well, a linear regression method was applied (Davidson et al., 1998). The emitted $\delta^{13}CH_4$ ($\delta^{13}CH_{4\_emit}$) for a chamber measurement period was obtained as the intercept of the Keeling plot (Figure S4c). The Keeling plot intercept (=$\delta^{13}CH_{4\_emit}$) was acquired from a simple linear regression line between $\delta^{13}CH_4$ and a reciprocal of CH_4 concentration in the headspace air. When the Keeling correlation was weak ($r < 0.20$, $p > 0.05$, $n > 66$) or the analyzer was not able to precisely measure the change in $\delta^{13}CH_4$ due to a too rapid change in CH_4 concentration triggered by bubble ebullitions, the value of $\delta^{13}CH_{4\_emit}$ was approximately estimated from the following mass balance equation (Krüger et al., 2002):

$$\delta^{13}CH_{4\_emit} = \left[\left(CH_{4\_end} \times \delta^{13}CH_{4\_end}\right) - \left(CH_{4\_ini} \times \delta^{13}CH_{4\_ini}\right)\right]/\left(CH_{4\_end} - CH_{4\_ini}\right) \tag{1}$$

where CH_{4_ini} and $\delta^{13}CH_{4\_ini}$ are the 1-min averages of the concentration (ppm) and $\delta^{13}C$ value of CH_4 in the chamber air, either at the start of the measurement (when analyzer in the HP mode) or up to 2.5 min before the start of measurement (when the analyzer was in the HR mode; see above). The CH_{4_end} and $\delta^{13}CH_{4\_end}$ are averages of the CH_4 concentration and $\delta^{13}CH_4$ in the head-space air for the last 1 min of a chamber measurement. The values of $\delta^{13}CH_{4\_emit}$ by the mass balance method agreed well with $\delta^{13}CH_{4\_emit}$ by the Keeling plot method using the plant chamber data sets which could obtain $\delta^{13}CH_{4\_emit}$ by both of the methods for most of the measurement period (Figure S5). Thus, we believe that the mass balance method is valid for estimating $\delta^{13}CH_{4\_emit}$.

2.4. Environmental Variables

Atmospheric pressure was measured with a barometer (MPXAZ6115A and MPXV7007DP, Freescale Inc., TX, USA), and air temperature was measured with a temperature sensor (HMP45A, Vaisala Inc., Helsinki, Finland). Soil temperatures were measured at 0, 3, 9, and 15 cm below the soil surface with type T thermocouples. Water depth above the soil surface was measured with a water level sensor (eTapeTM Continuous Fluid Level Sensor, Milone Technologies Inc., NJ, USA).

2.5. Analysis of Soil CH_4 Oxidation and Production

We estimated the CH_4 oxidation fraction of total soil CH_4 using the following mass balance equation with the in situ measured $\delta^{13}CH_4$, based on the assumption that total CH_4 in soil was mainly composed of CH_4 oxidation ($F_{ox(total)}$) and production ($1 - F_{ox(total)}$):

$$\delta^{13}CH_{4(total)} = F_{ox(total)} \times \delta^{13}CH_{4(oxidized)} + \left(1 - F_{ox(total)}\right) \times \delta^{13}CH_{4(prod)} \tag{2}$$

solved for $F_{ox(total)}$

$$F_{ox(total)} = \left(\delta^{13}CH_{4(total)} - \delta^{13}CH_{4(prod)}\right)/\left(\delta^{13}CH_{4(oxidized)} - \delta^{13}CH_{4(prod)}\right) \tag{3}$$

where $\delta^{13}CH_{4(total)}$ is the measured $\delta^{13}CH_4$ value of soil gases, $\delta^{13}CH_{4(prod)}$ is the $\delta^{13}C$ value of CH_4 produced and unoxidized in paddy soil, and $\delta^{13}CH_{4(oxidized)}$ is the $\delta^{13}C$ value of CH_4 oxidized by methanotrophs. The value of $\delta^{13}CH_{4(prod)}$ was assumed to be equivalent to $\delta^{13}CH_4$ values in emitted bubbles from the interrow soil because the released bubbles from the interrow soil were not thought to be affected by CH_4 oxidation, both due to rapid transportation from the soil without isotopic fractionation and low root availability in the interrow soil (Chanton, 2005). The value of $\delta^{13}CH_{4(oxidized)}$ was deduced from the following mass balance equation for $F_{ox(total)}$ (Tyler et al., 1997):

$$F_{ox(total)} = \left(\delta^{13}CH_{4(prod)} - \delta^{13}CH_{4(oxidized)}\right)/\left[\left(1/\alpha_{ox} - 1\right) \times \left(\delta^{13}CH_{4(oxidized)} + 1,000\right)\right] \tag{4}$$

solved for $\delta^{13}CH_{4(oxidized)}$ by assuming $F_{ox} = 1$,

$$\delta^{13}CH_{4(oxidized)} = \alpha_{ox} \times \left(\delta^{13}CH_{4(prod)} + 1,000\right) - 1,000 \tag{5}$$

where α_{ox} is the isotopic fractionation during the CH_4 oxidation process. Chanton et al. (2008) reported values of α_{ox} between 1.025 and 1.038 in landfill soil over a temperature range of 12–35°C, similar to

temperatures in anaerobic paddy soil. A similar α_{ox} range between 1.025 and 1.033 was also found in a Chinese paddy soil at 28.3°C (Zhang et al., 2013). Unfortunately, since we did not directly measure α_{ox} in this paddy soil, we estimated $\delta^{13}CH_{4(oxidized)}$ by using the two different α_{ox} values (=1.025 and 1.038), and then calculated $F_{ox(total)}$ at each depth in the planted and interrow soils. The values of $\delta^{13}CH_{4(total)}$, $\delta^{13}CH_{4(prod)}$, $\delta^{13}CH_{4(oxidized)}$, and $F_{ox(total)}$ on each sampling day are shown in Tables S2 and S3.

The net CH_4 production ($F_{prod} = 1$) in paddy soil is assumed to be mainly derived from acetate fermentation (F_{ac}) and H_2/CO_2 reduction ($1 - F_{ac}$) processes, allowing us to obtain the following mass balance equation (Conrad, 2005; Krüger et al., 2002; Tyler et al., 1997),

$$\delta^{13}CH_{4(prod)} = F_{ac} \times \delta^{13}CH_{4(acetate)} + (1 - F_{ac}) \times \delta^{13}CH_{4(H_2/CO_2)} \tag{6}$$

where $\delta^{13}CH_{4(acetate)}$ and $\delta^{13}CH_{4(H_2/CO_2)}$ are the $\delta^{13}C$ values of acetate-derived and H_2/CO_2-derived CH_4, respectively. $\delta^{13}CH_{4(prod)}$ is the $\delta^{13}C$ value of CH_4 produced in paddy soil. As stated above, the value of $\delta^{13}CH_4$ in emitted bubbles from interrow was assumed to represent the unoxidized and produced $\delta^{13}CH_4$ ($=\delta^{13}CH_{4(prod)}$). Values of $\delta^{13}CH_{4(acetate)}$ in Japanese and Italian rice paddy soils have been reported ranging between −37‰ to −43‰ (Krüger et al., 2002; Sugimoto & Wada, 1993). Since the F_{ac} values in our study did not largely vary from this $\delta^{13}CH_{4(acetate)}$ range of −37‰ to −43‰ (Table S4), the value of $\delta^{13}CH_{4(acetate)}$ was set as the average, −40‰. The values of F_{ac} on each sampling day are also shown in Table S4.

The value of $\delta^{13}CH_{4(H_2/CO_2)}$ was calculated through the following definitional equation for the carbon isotope fractionation factor (α_{CO_2/CH_4}),

$$\alpha_{CO_2/CH_4} = \left(\delta^{13}CO_{2(prod)} + 1,000\right) / \left(\delta^{13}CH_{4(H_2/CO_2)} + 1,000\right) \tag{7}$$

solved for $\delta^{13}CH_{4(H_2/CO_2)}$,

$$\delta^{13}CH_{4(H_2/CO_2)} = \left(\delta^{13}CO_{2(prod)} + 1,000\right) / \alpha_{(CO_2/CH_4)} - 1,000 \tag{8}$$

where $\delta^{13}CO_{2(prod)}$ is the $\delta^{13}C$ value of CO_2 produced in paddy soil. The $\delta^{13}CO_{2(prod)}$ values were assumed to be the $\delta^{13}CO_2$ value in the soil gas at each depth. The value of α_{CO_2/CH_4} in submerged paddy soil generally varies from 1.045 to 1.083 (Conrad, 2005; Fey et al., 2004; Sugimoto & Wada, 1993; Zhang et al., 2011, 2013). Given that some α_{CO_2/CH_4} can produce negative values of calculated F_{ac} at some depths, an appropriate range of α_{CO_2/CH_4} for estimating F_{ac} values of 0–1 at all depths was 1.057–1.083 in the planted soil, and 1.073–1.083 in the interrow soil (Figure S6). The α_{CO_2/CH_4} in a submerged paddy soil decreased from 1.083 to 1.076 as temperature rose from 10°C to 37°C (Fey et al., 2004). In our study, the mean soil temperature at 1–15 cm depth was around 30°C on the gas sampling days, so the value of α_{CO_2/CH_4} was set to be 1.078 at 30°C (Fey et al., 2004). Finally, the acetate fermentation fraction of the total soil CH_4 ($=F_{ac(total)}$) was determined by multiplying F_{ac} by ($1 - F_{ox(total)}$); presented and discussed in sections 3.2 and 4.1. The values of $\delta^{13}CO_{2(prod)}$, $\delta^{13}CH_{4(H_2/CO_2)}$, and $F_{ac(total)}$ on each sampling day are shown in Tables S5 and S6.

2.6. Wavelet Analysis

We used cross wavelet and wavelet coherence analysis that can suitably examine correlation between two nonstationary geophysical time series data sets at different time frequency (Torrence & Compo, 1998). The analysis helped us to identify any diel linkage between $\delta^{13}CH_{4\_emit}$, CH_4 flux, and potentially associated parameters such as soil temperature and atmospheric pressure. The wavelet coherence ($R_n^2(s)$), representing local correlation coefficients in time frequency space, is defined as,

$$R_n^2(s) = \frac{\left|S\left(s^{-1}W_n^{XY}(s)\right)\right|^2}{S\left(s^{-1}\left|W_n^X(s)\right|^2\right) \times S\left(s^{-1}\left|W_n^Y(s)\right|^2\right)} \tag{9}$$

where $W_n^{XY}(s)$ represents the cross wavelet spectrum of two time series data sets (X_n and Y_n). $W_n^X(s)$ and $W_n^Y(s)$ are the cross-wavelet power. S and s denote a smoothing operator and the time scale, respectively. Further definitions can be found in Grinsted et al. (2004). The statistical significance test for wavelet
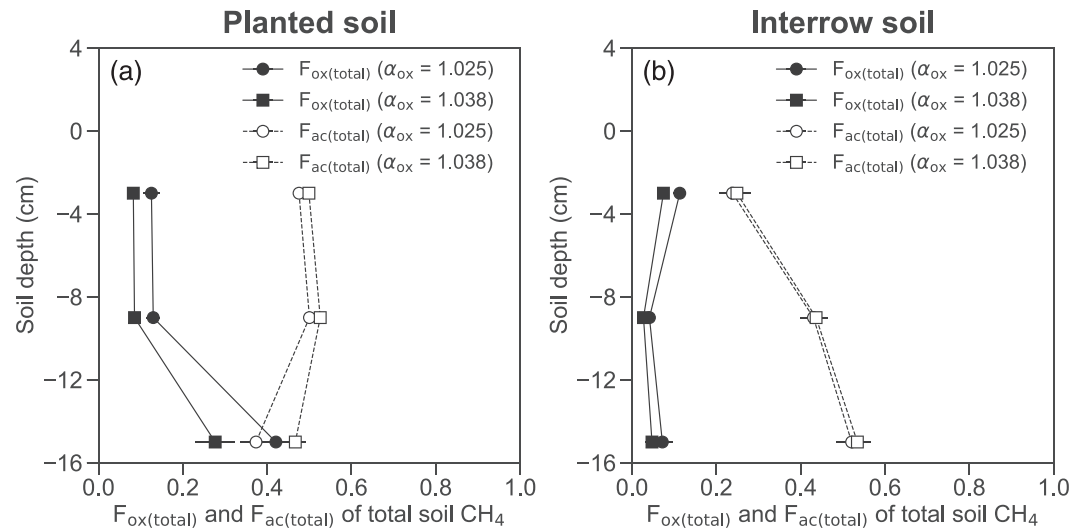
Figure 1. Depth profiles of CH_4 oxidation ($F_{ox(total)}$) and acetate fermentation ($F_{ac(total)}$) fractions of total CH_4 in the planted soil (a) and interrow soil (b). The values of $F_{ox(total)}$ were estimated by two previously reported α_{ox} values (=1.025 and 1.038). The $F_{ac(total)}$ values were calculated from the $F_{ox(total)}$ values. All values were averaged for four to five gas sampling days. The bars show one standard deviation ($n = 4$–5).

coherence was conducted using Monte Carlo methods according to Grinsted et al. (2004). We also estimated the time lag from the phase angle between the two time series data sets for statistically significant correlated periods. All wavelet analysis was performed using the freely available MatLab package developed by Grinsted et al. (2004) (available at https://sites.google.com/a/glaciology.net/grinsted/wavelet-coherence). Before implementing wavelet analysis, we first checked whether all measured time series data sets were normally distributed following Grinsted et al. (2004). The Shapiro-Wilk test showed that none of the time series data sets were normally distributed, so we transformed the raw time series data into the time series of percentiles following Grinsted et al. (2004). In addition, we gap-filled missing CH_4 flux and $\delta^{13}CH_{4\_emit}$ data because the wavelet analysis package does not accept time series data with missing values. Throughout the whole experimental period, the data gaps comprised 2.8% of the CH_4 flux and $\delta^{13}CH_{4\_emit}$ data for the plant chamber measurements and 2.5% of the equivalent water chamber measurements. To estimate the respective missing data we used the relationships found during the measurement period between CH_4 flux and soil surface temperature and between $\delta^{13}CH_{4\_emit}$ and soil surface temperature.

3. Results

3.1. Soil CH_4 Oxidation and Production Fractions

At each depth, there was little difference in the mean CH_4 oxidation fraction ($F_{ox(total)}$) estimated using either α_{ox} 1.025 or α_{ox} 1.038, except at 13–17 cm depth in the planted soil which had the highest $F_{ox(total)}$ values (Figure 1 and Table S3). The mean $F_{ox(total)}$ at each depth was higher in the planted soil than in the interrow soil (Figure 1). Based on these $F_{ox(total)}$ values (Figure 1 and Table S3), the fraction of CH_4 production ($F_{prod} = 1 - F_{ox(total)}$) in the paddy soil ranged between 0.58 and 0.97.

The estimated mean acetate fermentation fraction ($F_{ac(total)}$) values were also similar for α_{ox} 1.025 and 1.038 at each depth, except once again at 13–17 cm depth in the planted soil (Figure 1 and Table S6). The mean $F_{ac(total)}$ values at each depth were higher in the planted soil than in the interrow soil, except at 13–17 cm soil depth. Additionally, the $F_{ac(total)}$ values in the interrow soil increased with soil depth (Figure 1b).

The remaining fraction was assumed to be CH_4 production by H_2/CO_2 reduction $\left(F_{H_2/CO_{2(total)}} = 1 - F_{ac(total)} - F_{ox(total)}\right)$. This fraction was estimated to be higher at each depth in the interrow soil (1–5 cm depth: 0.65–0.68; 7–11 cm depth: 0.53; 13–17 cm depth: 0.41–0.42) than in the planted soil (1–5 cm depth: 0.39–0.42; 7–11 cm depth: 0.37–0.38; 13–17 cm depth: 0.21–0.25).
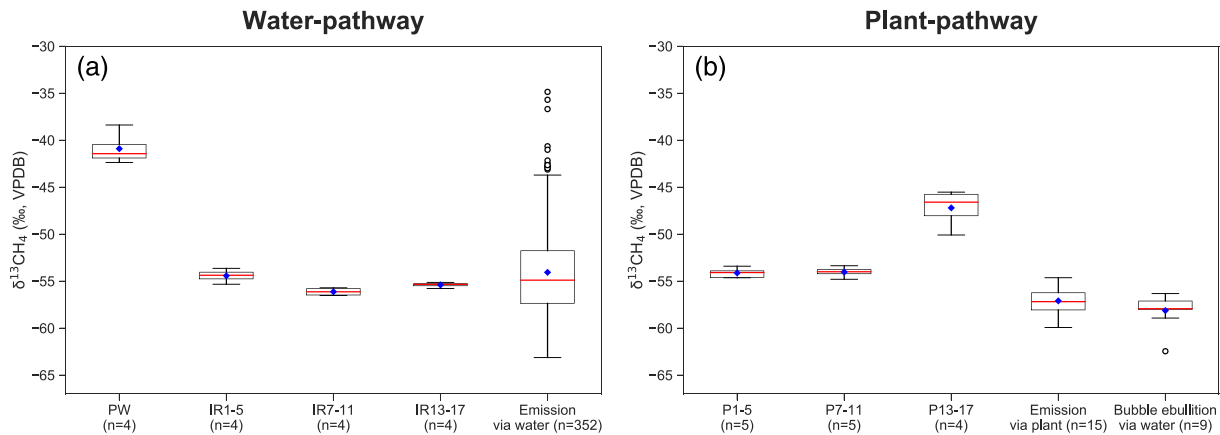
Figure 2. Boxplots of $\delta^{13}CH_4$ through the water and plant pathways. The red lines and blue diamonds in the boxes denote median and mean values, respectively. The open circles represent outliers. (a) Boxplot of $\delta^{13}CH_4$ in surface paddy water (PW), interrow soil at depths of 1–5 cm (IR1–5), 7–11 cm (IR7–11), and 13–17 cm (IR13–17), and emitted $\delta^{13}CH_4$ (=$\delta^{13}CH_{4\_emit}$) through the water pathway (emission via water) during the measurement period (=DOY 256 to 271). (b) Boxplot of planted soil $\delta^{13}CH_4$ at depths of 1–5 cm (P1–5), 7–11 cm (P7–11), and 13–17 cm (P13–17), $\delta^{13}CH_{4\_emit}$ through the plant pathway (emission via plant), and $\delta^{13}CH_{4\_emit}$ via bubble ebullition through the water pathway from DOY 256 to 271. Since the planted soil $\delta^{13}CH_4$ was assumed to vary during each day due to a diel change in root oxygen and perhaps exudate supplies (Badri & Vivanco, 2009; Cho et al., 2012; Colmer & Pedersen, 2008; Waters et al., 1989; Watt & Evans, 1999), the planted soil $\delta^{13}CH_4$ at each depth ($n = 4$–5) was compared with only the plant-mediated $\delta^{13}CH_{4\_emit}$ at 11:32 a.m. LT from DOY 256 to 271 ($n = 15$). In contrast, the lack of roots in the interrow soil meant little diel change in root oxygen and exudate supplies, so the interrow soil $\delta^{13}CH_4$ at each depth ($n = 4$) was assumed to be comparable with the water-mediated $\delta^{13}CH_{4\_emit}$ for the entire period ($n = 352$). The plant-mediated $\delta^{13}CH_{4\_emit}$ at 11:32 a.m. LT was also compared with the water-mediated $\delta^{13}CH_{4\_emit}$ through bubble ebullition observed at 11:50 a.m. LT from DOY 256 to 271 ($n = 9$) assuming no significant difference in $\delta^{13}CH_{4\_emit}$ due to the different timing (32 and 50 min past each hour) of the water and plant chamber measurements. The reason for the smaller number of samplers for water-mediated $\delta^{13}CH_{4\_emit}$ through bubble ebullition ($n = 9$) was because bubble ebullition was not observed in the water chamber on every measurement day.

3.2. Soil and Emitted $\delta^{13}CH_4$

The carbon isotopic values of CH_4 in the interrow soil at all the depths ranged from −56.5‰ to −53.6‰. These isotope values are similar to the emitted $\delta^{13}CH_4$ values (=$\delta^{13}CH_{4\_emit}$) through the water pathway throughout the entire measurement period, with an interquartile range between −57.4‰ and −51.8‰ (Figure 2a). Welch's t test showed that the interrow soil $\delta^{13}CH_4$ at 1–5 cm depth was not significantly different from the water-mediated $\delta^{13}CH_{4\_emit}$ (Figure 2a, $p > 0.4$). However, the $\delta^{13}CH_4$ values in the paddy water were significantly heavier than the water-mediated $\delta^{13}CH_{4\_emit}$ (Figure 2a, Welch's t test, $p < 0.001$).

In the planted soil, $\delta^{13}CH_4$ values at all depths were significantly heavier than the plant-mediated $\delta^{13}CH_{4\_emit}$ measured at the nearest equivalent sampling time (11:32 a.m. LT) on each day throughout the entire period (Figure 2b, Welch's t test, $p < 0.005$). The planted soil $\delta^{13}CH_4$ were compared with only the plant-mediated $\delta^{13}CH_{4\_emit}$ at 11:32 a.m. LT on each day because it was considered that the planted soil $\delta^{13}CH_4$ values may have changed throughout the day due to a diel change in root oxygen and perhaps exudate supplies (Badri & Vivanco, 2009; Cho et al., 2012; Colmer & Pedersen, 2008; Waters et al., 1989; Watt & Evans, 1999). This was not considered to be a problem in the interrow soil which did not have a high density of plant roots.

3.3. Diel Variation in CH_4 Transportation Through the Water and Plant Pathways
3.3.1. Mean Diel CH_4 Variations

Figure 3 shows mean diel variations in CH_4 flux and $\delta^{13}CH_{4\_emit}$ via the water and plant pathways, obtained from measured data throughout the whole period (Figures S1a, S1b, S1c, and S1d). Methane fluxes through paddy water increased from 7:50 a.m. LT, reaching a maximum value in the afternoon, followed by a decrease to a minimum early the following morning (Figure 3a). In contrast, the water-mediated $\delta^{13}CH_{4\_emit}$ displayed minimum values in the afternoon and subsequently increased during the night, reaching a maximum peak between 7:50 and 10:00 a.m. LT (Figure 3b). The antiphase variations between the water-mediated CH_4 flux and the $\delta^{13}CH_{4\_emit}$ established a significant negative correlation between the water-mediated $\log_{10}$-CH_4 flux and $\delta^{13}CH_{4\_emit}$ ($r = -0.77$; $p < 0.001$; Figure 3c). A significant negative correlation was observed in all the measurement data ($r = -0.57$; $p < 0.01$; $n = 352$; Figure S7a).
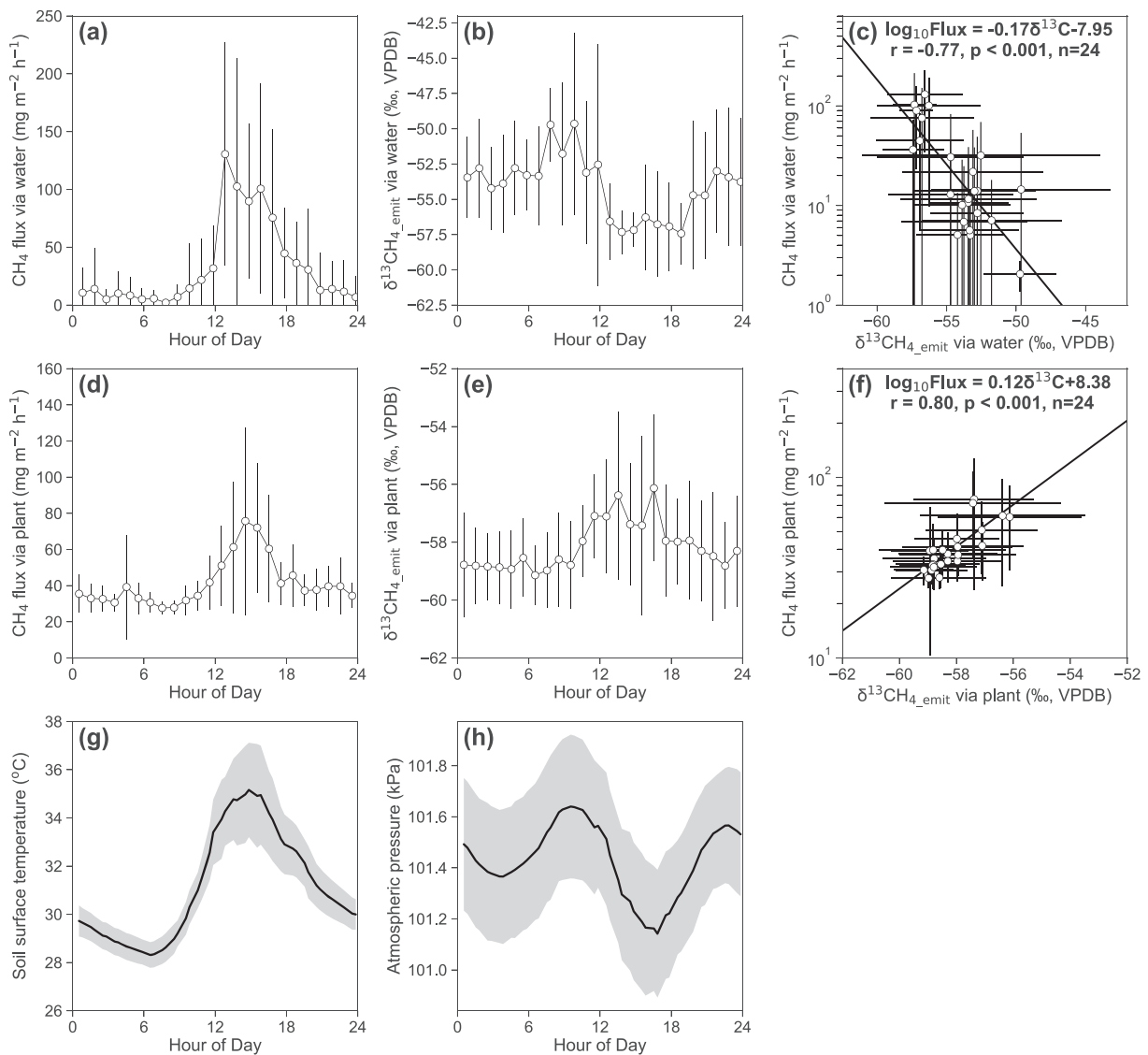
Figure 3. Mean diel variations in CH_4 flux, $\delta^{13}CH_{4\_emit}$, soil surface temperature, and atmospheric pressure in the water and plant pathways during the measurement period (DOY 256 to 271), plus relationships between CH_4 flux and $\delta^{13}CH_{4\_emit}$. (a) Mean diel variation in CH_4 flux via water. (b) Mean diel variation in $\delta^{13}CH_{4\_emit}$ via water. (c) Mean diel relationship between CH_4 flux and $\delta^{13}CH_{4\_emit}$ via water. (d) Mean diel variation in CH_4 flux via the plant. (e) Mean diel variation in $\delta^{13}CH_{4\_emit}$ via the plant. (f) Mean diel relationship between CH_4 flux and $\delta^{13}CH_{4\_emit}$ via the plant. (g) Mean diel variation in soil surface temperature. (h) Mean diel variation in atmospheric pressure. (a–f) The open circles and error bars represent the mean and one standard deviation of the data, respectively, measured at each hour ($n = 12$–15). (g–h) The solid lines and shaded area represent the mean and standard deviation, respectively, in each hour ($n = 15$).

The CH_4 fluxes through the plant pathway followed a similar pattern to those through the water pathway, with a maximum flux in the afternoon, followed by lower fluxes at night (Figure 3d). The plant-mediated $\delta^{13}CH_{4\_emit}$ also followed a similar diel pattern (Figure 3e), meaning there was a significant positive correlation between the plant-mediated $\log_{10}$-CH_4 flux and $\delta^{13}CH_{4\_emit}$ ($r = 0.80$; $p < 0.001$; Figure 3f). This corresponds to the results in previous studies (Chanton et al., 1997; Marik et al., 2002). A significant positive relationship between $\log_{10}$-CH_4 flux and $\delta^{13}CH_{4\_emit}$ through the plant pathway was also found for all the data throughout the measurement period ($r = 0.50$; $p < 0.01$; $n = 351$; Figure S7b).

The mean diel cycles in CH_4 fluxes through the two pathways closely matched the mean diel change in soil surface temperature, with an increase from the early morning to the afternoon, followed by a decrease at nighttime (Figures 3a, 3d, and 3g). The mean diel change in plant-mediated $\delta^{13}CH_{4\_emit}$ also closely matched that of soil surface temperature (Figures 3e and 3g), but water-mediated $\delta^{13}CH_{4\_emit}$ showed an

opposite pattern to soil surface temperature (Figures 3b and 3g). The diel variation in $\delta^{13}CH_{4\_emit}$ through the water pathway was more like the diel change in atmospheric pressure, with a minimum in the afternoon and a maximum in the early morning (Figures 3b and 3h). The mean diel pattern in atmospheric pressure was mostly converse to that for CH_4 flux through both the water and plant pathways, and also for plant-mediated $\delta^{13}CH_{4\_emit}$ (Figures 3a, 3d, 3e, and 3h).

3.3.2. Wavelet Coherence Results

The wavelet coherence analysis showed a significant antiphase coherence between the water-mediated CH_4 flux and $\delta^{13}CH_{4\_emit}$ at the daily timescale (Figure 4a). There was a 1.9-hr lag throughout most of the measurement period, obtained from the mean phase angle ($=-151.5°$) within the 5% significant region. This supports the significant negative relationship found between the mean diel log_{10}-CH_4 flux and $\delta^{13}CH_{4\_emit}$ through the water pathway (cf. section 3.3.1; Figure 3c). Moreover, throughout most of the measurement period, the $\delta^{13}CH_{4\_emit}$ through paddy water showed significant antiphase coherence with soil surface temperature, with a daily lag of 0.8 hr ($-168.0°$) (Figure 4c). This reflected the opposite diel patterns of water-mediated $\delta^{13}CH_{4\_emit}$ and soil temperature (Figures 3b and 3g). In contrast, there was a significant in-phase coherence at the daily timescale between the $\delta^{13}CH_{4\_emit}$ via the water pathway and atmospheric pressure, with only a 0.7-hr lag ($-10.9°$) (Figure 4e). This in-phase relationship was also consistent with the similar mean diel patterns of $\delta^{13}CH_{4\_emit}$ and atmospheric pressure (Figures 3b and 3h).

Unlike the water pathway, the plant pathway usually showed a significant in-phase relationship between CH_4 flux and $\delta^{13}CH_{4\_emit}$ at the daily timescale, with a 1.5-hr lag ($-22.6°$) throughout the measurement period (Figure 4b). This supports the significant positive correlation between the mean diel log_{10}-CH_4 flux and $\delta^{13}CH_{4\_emit}$ (Figure 3f). The plant-mediated $\delta^{13}CH_{4\_emit}$ also showed significant in-phase coherence with soil surface temperature, with a daily lag of only 0.6 hr ($-8.8°$), and antiphase coherence with atmospheric pressure when the daily lag was 2.1 hr ($148.9°$) (Figures 4d and 4f). The in-phase relationship between plant-mediated $\delta^{13}CH_{4\_emit}$ and soil temperature at the daily scale can also be seen from the mean diel variations in plant-mediated $\delta^{13}CH_{4\_emit}$ and soil temperature (Figures 3e and 3g). Similarly, the antiphase relationship between plant-mediated $\delta^{13}CH_{4\_emit}$ and atmospheric pressure can be seen from the mean diel variations in plant-mediated $\delta^{13}CH_{4\_emit}$ and atmospheric pressure (Figures 3e and 3h).

4. Discussion

4.1. CH_4 Processes in the Planted and Interrow Soils

4.1.1. Soil CH_4 Oxidation

The $F_{ox(total)}$ values indicate that there was higher CH_4 oxidation in the planted soil than in the interrow soil. This finding is also strongly suggested from the differences in soil gas concentrations and isotope signatures between the two soils (Text S1 and Figure S8). The results further indicate that the planted soil had more aerobic soil conditions, probably from root oxygen supplied via rice aerenchyma to the rhizosphere during the daytime (Cho et al., 2012; Colmer & Pedersen, 2008; Waters et al., 1989), and this increased CH_4 oxidation by methantrophic bacteria. In contrast, the lower root availability in the interrow soil would have reduced oxygen supply, resulting in more anaerobic conditions that would have reduced methantrophic bacteria activity.

The $F_{ox(total)}$ values in the paddy soil indicate that the greatest soil CH_4 oxidation by methanotrophic bacteria occurred in the planted soil at 13–17 cm depth. The highly active CH_4 oxidation at this depth was probably because of aerobic conditions due to high oxygen supply via rice roots. Root tips generally release oxygen more than the basal part of roots where barriers to radial oxygen loss (ROL) are developed (Armstrong, 1979, 2000; Nishiuchi et al., 2012), suggesting that there was a high density of root tips at 13–17 cm depth in the planted soil. The rice cultivar used in our study is assumed to have roots extending to 15–40 cm depth, with a high root density at 0–15 cm depth during the reproductive stage. Schmidt et al. (2011) and Atulba et al. (2015) have also confirmed that the root-oxidized area is developed at 10–20 cm depth during the rice reproductive stage. These results support the high distribution of rice root tips at 13–17 cm depth in the planted soil.

4.1.2. Soil CH_4 Production and Dominant Soil CH_4 Process

Methane production was the dominant CH_4 process in both paddy soils during the reproductive growth stage ($F_{prod} \geq 0.58$). Acetate fermentation ($F_{ac(total)}$) was occurring more actively in the planted soil than

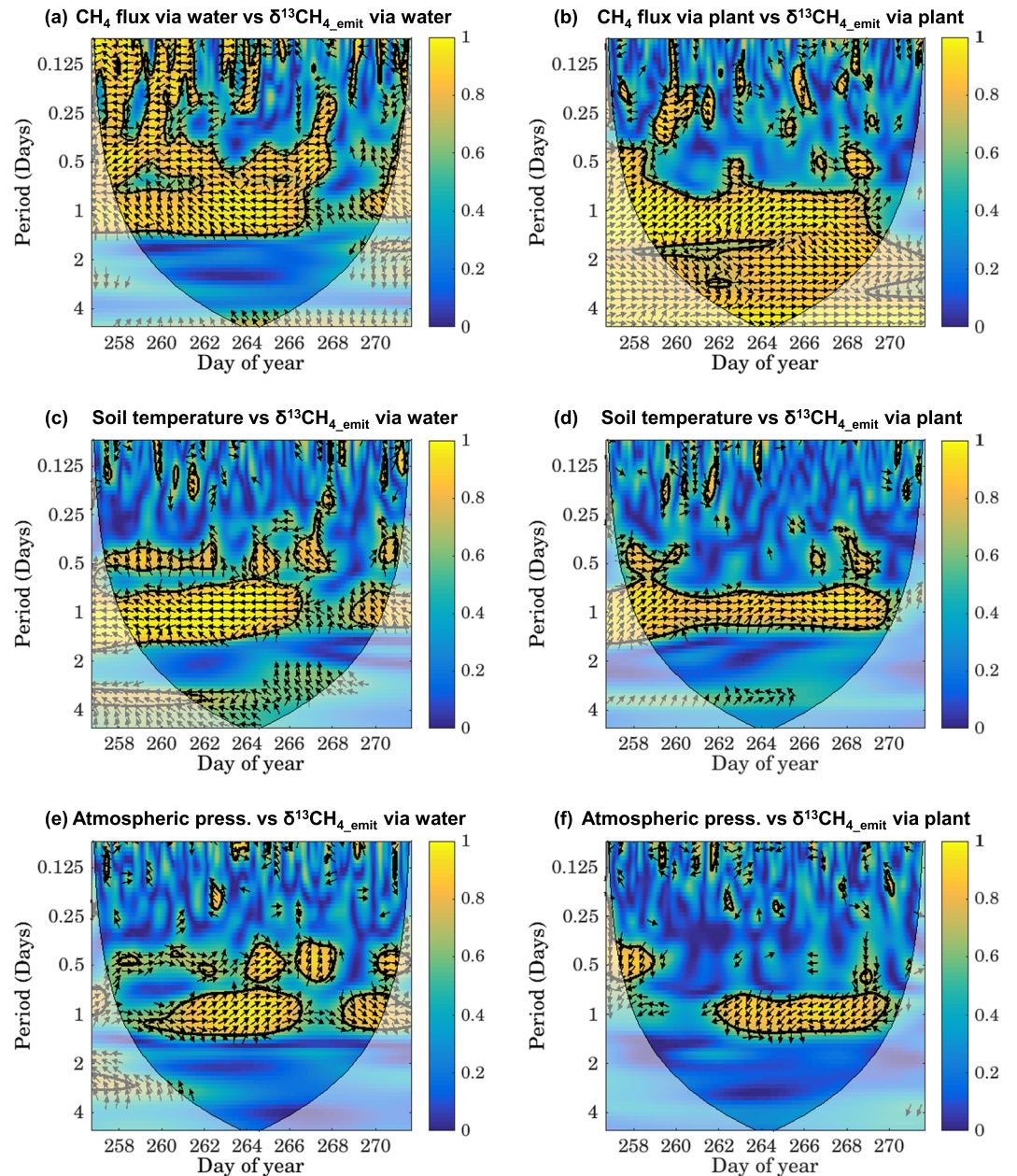**Figure 4.** Wavelet coherence of (a) CH$_4$ flux versus δ^{13}CH$_{4\_emit}$ via water, (b) CH$_4$ flux versus δ^{13}CH$_{4\_emit}$ via the plant, (c) soil surface temperature versus δ^{13}CH$_{4\_emit}$ via water, (d) soil surface temperature versus δ^{13}CH$_{4\_emit}$ via the plant, (e) atmospheric pressure versus δ^{13}CH$_{4\_emit}$ via water, and (f) atmospheric pressure versus δ^{13}CH$_{4\_emit}$ via the plant. The color represents the local coherence, corresponding to local correlation coefficients in time and frequency domains. The regions of significant coherence (at the 5% significance level determined using Monte Carlo methods) are the yellow regions enclosed by the thick black lines (Grinsted et al., 2004). Outside the cone of influence (the large cone shaped region bounded by the thin curved line), the wavelet transform suffers from edge effects (Grinsted et al., 2004). The black arrows in the water pathway plots indicate the phase angle relationship between the two time-series variables X (i.e., (a) CH$_4$ flux via water, (c) soil surface temperature, or (e) atmospheric pressure) and Y (δ^{13}CH$_{4\_emit}$ via water). The black arrows in the plant pathway plots indicate the phase angle relationship between the two time-series variables X (i.e., (b) CH$_4$ flux via the plant, (d) soil surface temperature, or (f) atmospheric pressure) and Y (δ^{13}CH$_{4\_emit}$ via the plant). Arrows pointing to the right without any phase shift signify the two variables are perfectly in-phase, whereas arrows pointing to the left without any phase shift mean they are perfectly antiphase. Arrows pointing vertically upward signify that Y leads X by 90° in in-phase. The lead of 90° can also be interpreted as Y lagging X by 270° in in-phase or Y lagging X by 90° in antiphase. The phase angles of the arrows increase in a clockwise direction and signify the time lag between the X and Y variables, dependent on the time period (y-coordinate) (e.g., 90° at the 1-day time period = 6-hr lag at the daily timescale). Further information can be found in Grinsted et al. (2004).
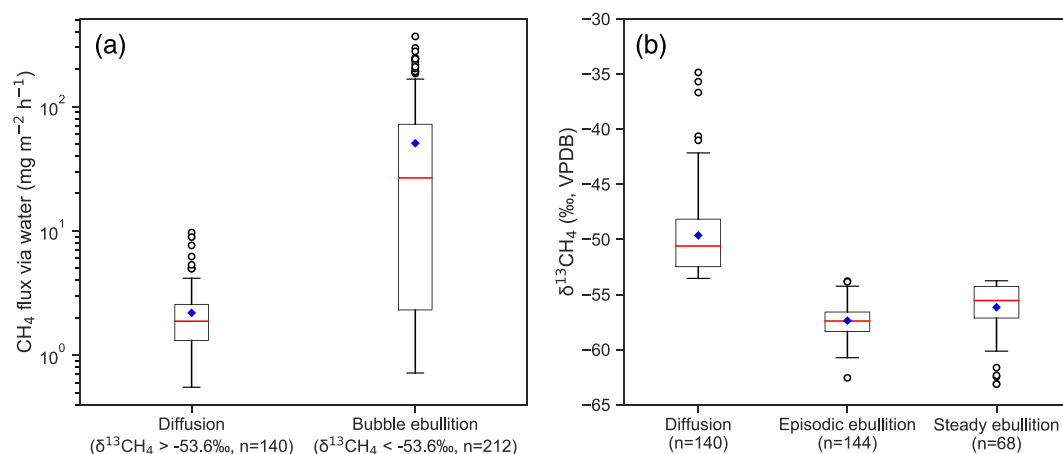
Figure 5. (a) Boxplot of water-mediated CH_4 flux via diffusion and bubble ebullition during the measurement period (DOY 256–271). The water pathway was classified into diffusion and bubble ebullition based on the threshold of emitted $\delta^{13}CH_4$ via water (=−53.6‰) (i.e., diffusion: $\delta^{13}CH_{4\_emit} > −53.6$‰, bubble ebullition: $\delta^{13}CH_{4\_emit} < −53.6$‰). The threshold of emitted $\delta^{13}CH_4$ via water represents the upper value of interrow soil $\delta^{13}CH_4$ (=−53.6‰) with the assumption that the bubble ebullition process emits similar or lighter $\delta^{13}CH_4$ than soil $\delta^{13}CH_4$. (b) Boxplot of water-mediated $\delta^{13}CH_4$ via diffusion, episodic ebullition, and steady ebullition from DOY 256 to 271. The bubble ebullition was divided into episodic and steady ebullition on the basis of the threshold of CH_4 flux rates (=5 mg m^{-2} hr^{-1}) (i.e., episodic ebullition: CH_4 flux > 5 mg m^{-2} hr^{-1}, steady ebullition: CH_4 flux < 5 mg m^{-2} hr^{-1}). The red lines and blue diamonds in the boxes denote median and mean values, respectively. The open circles represent outliers.

in the interrow soil at 1–11 cm depths, probably due to acetate supply from rice roots enhancing acetoclastic methanogens in the planted rhizosphere soil (Hayashi et al., 2015; Lee et al., 2015; Schütz et al., 1989). In contrast, the low root availability in the interrow soil would have limited root acetate supply, which would explain the larger contribution of H_2/CO_2 reduction $\left(F_{H_2/CO_{2(total)}} \geq 0.53\right)$ to CH_4 production at these depths.

However, at 13–17 cm depth in the interrow soil acetate fermentation was more dominant than H_2/CO_2 reduction ($F_{ac(total)} > 0.5$). This suggests that there were more acetoclastic methanogens available in the deeper paddy soil, as has also been found by Lee et al. (2015). In contrast, the CH_4 production from acetate fermentation in the planted soil was lower at 13–17 cm depth than at 1–11 cm depth. This was probably due to the more aerobic conditions in the planted soil at that depth (see section 4.1.1) reducing the activity of acetoclastic methanogens.

4.2. CH_4 Transportation Via Water
4.2.1. Water-Mediated CH_4 Transportation Partitioning
The lack of any significant difference in $\delta^{13}CH_4$ between the interrow soil CH_4 at 1–5 cm depth and CH_4 emission via the water pathway indicates that most of the observed CH_4 emission through the water pathway was derived from bubble ebullition. This is because bubble ebullition generally does not cause any large isotopic fractionation during the transportation from the soil to the atmosphere (i.e., $\delta^{13}CH_{4\_emit} \approx$ soil $\delta^{13}CH_4$) (Chanton, 2005), whereas diffusion generally causes isotopic fractionation during gas transport, which would result in heavier $\delta^{13}CH_{4\_emit}$ than soil $\delta^{13}CH_4$ (Chanton, 2005; Happell et al., 1994). Although hydrodynamic transport, which is involved in the diffusion process, is assumed to cause less isotopic fractionation than molecular diffusion, it would still produce more isotopic discrimination than bubble ebullition.

Assuming that the bubble ebullition process emitted $\delta^{13}CH_4$ that was similar or lighter than the soil $\delta^{13}CH_4$, we divided the water-mediated CH_4 emission for each chamber measurement into bubble ebullition ($\delta^{13}CH_{4\_emit} < −53.6$‰) and diffusion ($\delta^{13}CH_{4\_emit} > −53.6$‰) processes by using the maximum interrow soil $\delta^{13}CH_4$ (=−53.6‰) as the upper limit for bubble ebullition (Figure 5a). The diffusion process, including hydrodynamic transport, was assumed to release heavier $\delta^{13}CH_4$ than soil $\delta^{13}CH_4$ due to the influence of isotopic fractionation by diffusion and CH_4 oxidation at the soil-water interface (Chanton, 2005).

There was usually only a gradual increase in CH_4 concentration during a chamber closure period due to diffusion ($\delta^{13}CH_{4\_emit} > -53.6‰$), with almost all CH_4 flux rates of less than 5 mg m^{-2} hr^{-1}, significantly lower than bubble ebullition (Figure 5a, Welch's t test, $p < 0.001$). The upper value of the diffusive CH_4 flux rate (5 mg m^{-2} hr^{-1}) agrees with the mean diffusive CH_4 flux rate at the water-atmosphere interface in a flooded fen site (Hoffmann et al., 2017), so the value was considered as the upper threshold diffusive CH_4 flux rate. Furthermore, in another flooded wetland study (Poindexter et al., 2016), the maximum diffusive CH_4 flux rate by hydrodynamic transport was 200 nmol m^{-2} s^{-1} (=11.52 mg m^{-2} hr^{-1}), which covers the maximum outlier diffusive CH_4 flux rates in our study (Figure 5a). Therefore, these wetland field data support the division between diffusion and bubble ebullition based on soil $\delta^{13}CH_4$ (=$-53.6‰$).

In contrast, bubble ebullition ($\delta^{13}CH_{4\_emit} < -53.6‰$) usually produced CH_4 flux rates higher than the maximum limit for CH_4 diffusion (=5 mg m^{-2} hr^{-1}) (Figure 5a). Bubble ebullition is mainly classified into episodic and steady ebullitions (Coulthard et al., 2009; Green, 2013). The episodic ebullition process rapidly releases bubbles from the soil into the atmosphere and therefore usually shows high CH_4 flux rates (Komiya et al., 2015; Tokida et al., 2007), which suggests that most of the measured bubble ebullition in our study was derived from episodic ebullition.

However, sometimes in our study bubble ebullition ($\delta^{13}CH_{4\_emit} < -53.6‰$) also displayed low CH_4 flux rates like those via diffusion (CH_4 flux < 5 mg m^{-2} hr^{-1}) (Figure 5a). Steady ebullition is considered to cause a steady stream of small bubbles, leading to a gradual increase in CH_4 concentration (Coulthard et al., 2009; Goodrich et al., 2011; Green, 2013), which indicates that the low CH_4 flux rates by bubble ebullition (<5 mg m^{-2} hr^{-1}) in our study were most likely derived from steady ebullition. Therefore, we divided the bubble ebullition ($\delta^{13}CH_{4\_emit} < -53.6‰$) into two types: episodic ebullition with CH_4 flux rates >5 mg m^{-2} hr^{-1} and steady ebullition with CH_4 flux rates <5 mg m^{-2} hr^{-1} (Figure 5b).

During the study period, episodic ebullition, steady ebullition, and diffusion were confirmed as the respective dominant CH_4 emission pathways in 40.9%, 19.3%, and 39.8% of the water chamber measurements ($n = 352$) (Figure 5b). Episodic ebullition was the predominant pathway during high CH_4 emissions from paddy water (CH_4 flux >5 mg m^{-2} hr^{-1}), whereas the diffusion process was the dominant pathway during low CH_4 emission via water (CH_4 flux <5 mg m^{-2} hr^{-1}). The low contribution of steady ebullition may have been due to the influence of CH_4 oxidation on small CH_4 bubbles as they gradually passed through the soil-water surface (Green, 2013).

4.2.2. From Which Soil Depth Are Bubbles Released Via Water?

The $\delta^{13}CH_{4\_emit}$ via steady ebullition was similar to the interrow soil $\delta^{13}CH_4$ at 7–11 cm depth (Figures 2a and 5b, Welch's t test, $p > 0.9$). This indicates that bubbles released via steady ebullition originated from 7–11 cm soil depth. In contrast, the $\delta^{13}CH_{4\_emit}$ via episodic ebullition was significantly lighter than the interrow soil $\delta^{13}CH_4$ at any depth (Figures 2a and 5b, Welch's t test, $p < 0.005$). This would suggest that the episodic ebullition process released bubbles from below 17 cm soil depth. However, clay paddy soil is not very porous, so it is unlikely that episodic ebullition could rapidly and smoothly release bubbles from deep soil (below 17 cm) into the atmosphere. Also, episodic ebullition releases bubbles rapidly from the soil meaning it is possible that the gas samplers in our study did not have enough time to adequately equilibrate with the soil gas and so accurately detect the carbon isotopic signal of CH_4 in the rapidly released bubbles. Based on the points in the previous sentences, it is more likely that the bubbles emitted via episodic ebullition were actually expanded from small bubbles in the soil. These small bubbles were mainly produced at 7–11 cm depth and then transferred to the soil surface layer and then the atmosphere. In the afternoon the soil temperature in the surface soil (e.g., 0–7 cm) increased more sharply than in deeper soil (Figure S9), and this probably would have enabled the small bubbles in the shallower soil to expand more easily, which would have triggered the episodic ebullition.

4.2.3. Diel CH_4 Transportation Via Water (Bubble Ebullition and Diffusion)

The wavelet analysis results indicate that diel CH_4 transportation through the water pathway was significantly related to diel variations in soil surface temperature and atmospheric pressure. As discussed in section 4.2.1, there are three main CH_4 emission pathways via paddy water: episodic ebullition, steady ebullition, and diffusion. Based on $\delta^{13}CH_{4\_emit}$ and CH_4 flux, we apportioned the number of times that each of the three CH_4 emission pathways was the dominant pathway contributing to the total CH_4 in each hourly water chamber measurement (Figure 6).
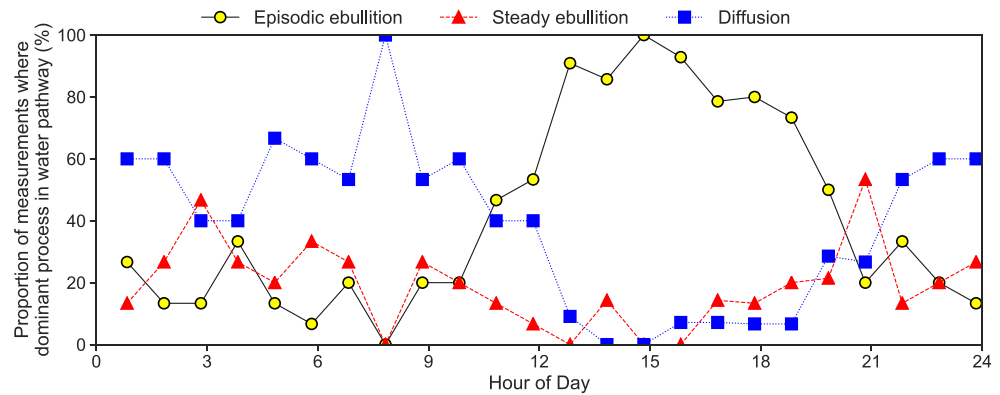
Figure 6. Diel variations in numbers of times that episodic ebullition ($\delta^{13}CH_{4\_emit} < -53.6‰$ and CH_4 flux > 5 mg m^{-2} hr^{-1}), steady ebullition ($\delta^{13}CH_{4\_emit} < -53.6‰$ and CH_4 flux < 5 mg m^{-2} hr^{-1}) and diffusion ($\delta^{13}CH_{4\_emit} > -53.6‰$) were the dominant pathway contributing to the total water chamber CH_4 for each hour during the measurement period (DOY 256–271).

Episodic ebullition ($\delta^{13}CH_{4\_emit} < -53.6‰$, CH_4 flux > 5 mg m^{-2} hr^{-1}) frequently occurred in the afternoon when the soil surface temperature increased and atmospheric pressure decreased (Figures 3a, 3b, 3g, 3h, and 6). The increase in soil temperature from the morning to afternoon was also observed at 3, 9, and 15 cm soil depths (Figure S9). The daytime changes in both soil temperature and atmospheric pressure would have enhanced bubble size and thus bubble buoyancy, which probably triggered the frequent episodic ebullitions (Fechner-Levy & Hemond, 1996; Kellner et al., 2006; Komiya et al., 2015; Tokida et al., 2009).

In contrast, diffusion ($\delta^{13}CH_{4\_emit} > -53.6‰$) and steady ebullition ($\delta^{13}CH_{4\_emit} < -53.6‰$, CH_4 flux < 5 mg m^{-2} hr^{-1}) were more dominant during the night (Figures 3a, 3b, and 6), when lower soil temperature and higher atmospheric pressure probably diminished episodic ebullitions (Figures 3a, 3b, 3g, 3h, and 6). In addition, the small drop in atmospheric pressure from 10:50 p.m. to 3:50 a.m. LT probably contributed to frequent steady ebullition of small bubbles (Figures 3a, 3b, 3h, and 6). Diffusion dominated at 7:50 a.m. LT when the soil temperature was lowest and the atmospheric pressure was near its peak (Figures 3a, 3b, 3h, and 6), which would have likely reduced bubble ebullition (i.e., episodic and steady ebullition).

4.3. CH$_4$ Transportation Via Plants
4.3.1. From Which Soil Depth Is Methane Released Via Rice Plants?

The plant-mediated $\delta^{13}CH_{4\_emit}$, measured at 11:32 a.m. LT, was significantly different from the planted soil $\delta^{13}CH_4$ at all the depths, but not significantly different from the water-mediated $\delta^{13}CH_{4\_emit}$ by bubble ebullition at the nearest equivalent time (11:50 a.m. LT) (Figure 2b, Welch's t test, $p > 0.17$). The water-mediated $\delta^{13}CH_{4\_emit}$ by bubble ebullition normally represents bubble $\delta^{13}CH_4$ in the soil (i.e., emitted bubble $\delta^{13}CH_{4\_emit} \approx$ soil bubble $\delta^{13}CH_4$). Therefore, these results indicate that, at least around the noon chamber measurement time, the rice plants transported CH_4 in bubbles from the paddy soil through the plant aerenchyma into the atmosphere without any large isotope fractionation.

To further examine whether the rice plants transported methane in bubbles at other times, we compared $\delta^{13}CH_{4\_emit}$ values between the plant and water pathways at each hour of the day (plant and water chamber measurements at 32 and 50 min past each hour, respectively) (Figure 7). There was no significant difference in $\delta^{13}CH_{4\_emit}$ between the plant and water pathways from 11:32 a.m. to 6:50 p.m. LT when bubble ebullition dominated the water pathway, as discussed in section 4.2.3 (emitted bubble $\delta^{13}CH_{4\_emit} \approx$ soil bubble $\delta^{13}CH_4$) (Figure 7, Welch's t test, $p > 0.05$). This finding strongly suggests that methane emitted through the plant pathway in the afternoon originated from CH_4 in soil bubbles, just like at noon. The bubbles were mainly produced at 7–11 cm depth and expanded in the afternoon throughout 0–11 cm depth (cf. section 4.2.3). This indicates that rice roots could easily come into contact with the expanded bubbles at 0–11 cm and then transfer methane in the bubbles through the rice aerenchyma into the atmosphere. Therefore, the CH_4 emitted through rice plants in the afternoon was probably derived from the expanded bubbles at 0–11 cm depth. This soil depth was also the site with the highest CH_4 production fraction area in the planted soil (i.e., 1–11 cm soil depth, $F_{prod} > 0.87$, Figure 1).
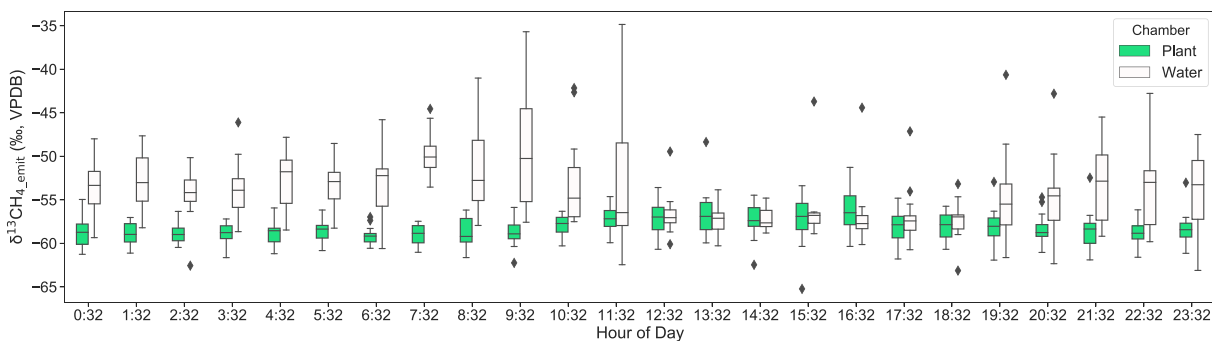
Figure 7. Boxplot of diel variations in water- and plant-mediated $\delta^{13}CH_{4\_emit}$ during the measurement period (DOY 256–271). The plant and water chamber measurements were conducted at 32 and 50 min, respectively, past each hour. The values for water- and plant-mediated $\delta^{13}CH_{4\_emit}$ were compared for each hour assuming no significant difference in $\delta^{13}CH_{4\_emit}$ due to the different timing (32 and 50 min past each hour) of the water and plant chamber measurements. The black diamonds represent outliers.

4.3.2. Diel CH₄ Transportation Via Plants

The wavelet analysis results indicate that diel variations in soil surface temperature and atmospheric pressure significantly affected diel CH_4 transportation through the plant pathway. As discussed in section 4.3.1, rice plants transported methane in expanded bubbles in the afternoon. The bubble expansion mainly stemmed from both the increase in soil temperature and the decrease in atmospheric pressure in the afternoon (cf. section 4.2.3), which also helped the bubbles to come in contact with the rice roots. There is generally a larger amount of CH_4 in bubbles than in soil solution, because of insolubility (Himmelblau, 1964; Tokida et al., 2013). In addition, methane in bubbles can diffuse much faster than CH_4 in soil solution (Himmelblau, 1964; Tokida et al., 2013). Therefore, large amounts of CH_4 in expanded bubbles would have transferred into the rice plants. Then, once in the plant the CH_4 gas would move diffusively through the rice plant arenchyma (Chanton et al., 1997). In the daytime the rise in soil temperature and decrease in atmospheric pressure would probably have enhanced gas diffusive transport, following the Chapman-Enskog diffusion theory. Hosono and Nouchi (1998) found that CH_4 emission increased with increasing diffusive conductance of rice plants for CH_4 due to the increase in soil temperature. Therefore, the afternoon temperature and atmospheric pressure conditions would have enhanced diffusive CH_4 transport through the rice plants and resulted in an increase in CH_4 flux. The enhanced plant-mediated CH_4 transportation in the afternoon probably contributed to the lack of any significant isotopic difference between the CH_4 emitted through the rice plants and soil bubble CH_4 (cf. section 4.3.1).

In contrast, at night both the low soil temperature and high atmospheric pressure probably diminished the nighttime bubble expansion in the soil (cf. section 4.2.3). This probably made it more difficult for CH_4-rich bubbles to come into contact with roots, thereby reducing nighttime CH_4 transport from bubbles through rice plants to the atmosphere. Furthermore, the soil temperature and atmospheric pressure conditions at night also probably decreased the diffusive CH_4 transportation through rice plants, following the Chapman-Enskog diffusion theory. Since the light carbon isotope ($=^{12}CH_4$) can move faster than the heavy one ($=^{13}CH_4$), the reduced plant-mediated diffusive transportation at night would probably have transported $^{12}CH_4$ more easily than $^{13}CH_4$, which would explain the lighter value of the plant-mediated $\delta^{13}CH_{4\_emit}$ at night.

Collectively, the above discussion regarding plant-mediated CH_4 transportation shows that the diel changes in soil temperature and atmospheric pressure mainly regulated the diel variations in bubble expansion in the soil and plant-mediated CH_4 diffusion, both of which drove the diel variations in the plant-mediated CH_4 transport. The subsequent wavelet analysis of the water-mediated CH_4 flux and plant-mediated $\delta^{13}CH_{4\_emit}$ also confirmed a significant in-phase coherency at the daily timescale, with a lag of 0.7 hr (9.8°) (Figure S10). Since the diel CH_4 emission through the water pathway was mainly regulated by soil bubble expansion, the wavelet coherence results also support the theory that diel change in CH_4 bubble expansion in soil is a key diel controller of plant-mediated CH_4 transportation.

5. Summary and Conclusions

We examined the CH_4 oxidation, production, and transportation processes at both the soil-plant-atmosphere and soil-water-atmosphere interfaces during the reproductive growth period of tropical paddy rice using natural $\delta^{13}CH_4$ and $\delta^{13}CO_2$. Our results reveal that more CH_4 oxidation and production by acetate fermentation occurred in the planted soil compared with the interrow soil, due to increased oxygen and organic matter supply through rice roots in the planted soil. Furthermore, we found that the acetate fermentation was the dominant soil CH_4 process in the planted soil except at 13–17 cm depth where active CH_4 oxidation occurred. In contrast, the H_2/CO_2 reduction was the dominant CH_4 process in the interrow soil, except at 13–17 cm depth where the acetate fermentation occurred more actively.

Assessing both CH_4 flux and emitted $\delta^{13}CH_4$ through the water pathway showed that methane in the interrow soil moved upward into the atmosphere by three transportation modes: episodic ebullition, steady ebullition, and diffusion at the water-atmosphere interface. Episodic and steady ebullitions released bubbles mainly from 7–11 cm soil depth. In addition, high CH_4 emissions (>5 mg m^{-2} hr^{-1}) through the paddy water were dominated by episodic ebullition, whereas low (<5 mg m^{-2} hr^{-1}) emissions were dominated by diffusion. The water pathway showed a significant negative correlation between the mean diel CH_4 flux and emitted $\delta^{13}CH_4$; this negative relationship was identified throughout most of the measurement period by the wavelet coherence analysis. The diel variations in CH_4 flux and emitted $\delta^{13}CH_4$ through the water pathway showed that episodic bubble ebullitions dominated the water-mediated CH_4 transportation in the daytime, whereas diffusion dominated the water pathway at night. The daily variations in episodic ebullition, steady ebullition, and diffusion were mainly regulated by the diel changes in soil temperature and atmospheric pressure.

In contrast, the plant pathway showed a significant positive correlation between the mean diel CH_4 flux and emitted $\delta^{13}CH_4$. Comparison of the mean diel emitted $\delta^{13}CH_4$ by the water and plant pathways revealed that the rice plants transported CH_4 in bubbles, developed at 0–11 cm depth. The key factors for regulating the diel variation in CH_4 transportation through rice plants were changes in bubble expansion and plant-mediated CH_4 diffusion, regulated by diel changes in soil temperature and atmospheric pressure.

These results demonstrate that the diel pattern of CH_4 transportation through the plant pathway is strongly related to diel change in bubble expansion in soil. Better understanding of diel and longer-term changes in CH_4 bubbles in paddy soil would help to improve our knowledge of the temporal changes in CH_4 flux, and prediction of the CH_4 budget in rice paddies. This perspective is also important for other wetland field studies that have similar characteristics to rice paddies.

Conflict of Interest

The authors declare having no conflict of interest.

Data Availability Statement

All the data in this paper and supporting information are available online (https://dx.doi.org/10.17617/3.4o).

References

Armstrong, W. (1979). Aeration in higher plants. *Advances in Botanical Research*, 7, 225–332. https://doi.org/10.1016/S0065-2296(08)60089-0

Armstrong, W. (2000). Oxygen distribution in wetland plant roots and permeability barriers to gas-exchange with the rhizosphere: A microelectrode and modelling study with Phragmites australis. *Annals of Botany*, *86*(3), 687–703. https://doi.org/10.1006/anbo.2000.1236

Atulba, S. L., Gutierrez, J., Kim, G. W., Kim, S. Y., Khan, M. I., Lee, Y. B., & Kim, P. J. (2015). Evaluation of rice root oxidizing potential using digital image analysis. *Journal of Korean Society for Applied Biological Chemistry*, *58*(3), 463–471. https://doi.org/10.1007/s13765-015-0042-x

Badri, D. V., & Vivanco, J. M. (2009). Regulation and function of root exudates. *Plant, Cell & Environment*, *32*(6), 666–681. https://doi.org/10.1111/j.1365-3040.2009.01926.x

Bilek, R. S., Tyler, S. C., Sass, R. L., & Fisher, F. M. (1999). Differences in CH_4 oxidation and pathways of production between rice cultivars deduced from measurements of CH_4 flux and $\delta^{13}C$ of CH_4 and CO_2. *Global Biogeochemical Cycles*, *13*(4), 1029–1044. https://doi.org/10.1029/1999GB900040

Bindoff, N. L., Stott, P. A., AchutaRao, K. M., Allen, M. R., Gillett, N., Gutzler, D., et al. (2013). Detection and attribution of climate change: From global to regional. In T. F. Stocker, D. Qin, G.-K. Plattner, et al. (Eds.), *Climate change 2013—The physical science basis, Working Group I Contribution to the Fifth Assessment Report of the Intergovernmental Panel on Climate Change* (pp. 867–952). Cambridge, UK, and New York: Cambridge University Press. https://doi.org/10.1017/CBO9781107415324.022

Bridgham, S. D., Cadillo-Quiroz, H., Keller, J. K., & Zhuang, Q. (2013). Methane emissions from wetlands: Biogeochemical, microbial, and modeling perspectives from local to global scales. *Global Change Biology*, *19*(5), 1325–1346. https://doi.org/10.1111/gcb.12131

Butterbach-Bahl, K., Papen, H., & Rennenberg, H. (1997). Impact of gas transport through rice cultivars on methane emission from rice paddy fields. *Plant, Cell and Environment*, *20*(9), 1175–1183. https://doi.org/10.1046/j.1365-3040.1997.d01-142.x

Chanton, J. P. (2005). The effect of gas transport on the isotope signature of methane in wetlands. *Organic Geochemistry*, *36*(5), 753–768. https://doi.org/10.1016/j.orggeochem.2004.10.007

Chanton, J. P., Powelson, D. K., Abichou, T., Fields, D., & Green, R. (2008). Effect of temperature and oxidation rate on carbon-isotope fractionation during methane oxidation by landfill cover materials. *Environmental Science & Technology*, *42*(21), 7818–7823. https://doi.org/10.1021/es801221y

Chanton, J. P., Whiting, G. J., Blair, N. E., Lindau, C. W., & Bollich, P. K. (1997). Methane emission from rice: Stable isotopes, diurnal variations, and CO_2 exchange. *Global Biogeochemical Cycles*, *11*(1), 15–27. https://doi.org/10.1029/96GB03761

Cho, R., Schroth, M. H., & Zeyer, J. (2012). Circadian methane oxidation in the root zone of rice plants. *Biogeochemistry*, *111*(1–3), 317–330. https://doi.org/10.1007/s10533-011-9651-6

Colmer, T., & Pedersen, O. (2008). Oxygen dynamics in submerged rice (Oryza sativa). *The New Phytologist*, *178*(2), 326–334. https://doi.org/10.1111/j.1469-8137.2007.02364.x

Conrad, R. (2005). Quantification of methanogenic pathways using stable carbon isotopic signatures: A review and a proposal. *Organic Geochemistry*, *36*(5), 739–752. https://doi.org/10.1016/j.orggeochem.2004.09.006

Coulthard, T. J., Baird, A. J., Ramirez, J., & Waddington, J. M. (2009). Methane dynamics in peat: Importance of shallow peats and a novel reduced-complexity approach for modeling ebullition. *Geophysical Monograph Series*, *184*, 173–185. https://doi.org/10.1029/2008GM000811

Davidson, E. A., Belk, E., & Boone, R. D. (1998). Soil water content and temperature as independent or confounded factors controlling soil respiration in a temperate mixed hardwood forest. *Global Change Biology*, *4*(2), 217–227. https://doi.org/10.1046/j.1365-2486.1998.00128.x

de Mello, W. Z., & Hines, M. E. (1994). Application of static and dynamic enclosures for determining dimethyl sulfide and carbonyl sulfide exchange in Sphagnum peatlands: Implications for the magnitude and direction of flux. *Journal of Geophysical Research*, *99*(D7), 14601. https://doi.org/10.1029/94JD01025

FAOSTAT (2018). *Crops: Rice, paddy*. Rome, Italy: Food and Agriculture Organization of the United Nations. Retrieved from http://www.fao.org/faostat/en/#data/QC

Fechner-Levy, E. J., & Hemond, H. F. (1996). Trapped methane volume and potential effects on methane ebullition in a northern peatland. *Limnology and Oceanography*, *41*(7), 1375–1383. https://doi.org/10.4319/lo.1996.41.7.1375

Fey, A., Claus, P., & Conrad, R. (2004). Temporal change of ^{13}C-isotope signatures and methanogenic pathways in rice field soil incubated anoxically at different temperatures. *Geochimica et Cosmochimica Acta*, *68*(2), 293–306. https://doi.org/10.1016/S0016-7037(03)00426-5

Goodrich, J. P., Varner, R. K., Frolking, S., Duncan, B. N., & Crill, P. M. (2011). High-frequency measurements of methane ebullition over a growing season at a temperate peatland site. *Geophysical Research Letters*, *38*, L07404. https://doi.org/10.1029/2011GL046915

Green, S. M. (2013). Ebullition of methane from rice paddies: The importance of furthering understanding. *Plant and Soil*, *370*(1–2), 31–34. https://doi.org/10.1007/s11104-013-1790-1

Grinsted, A., Moore, J. C., & Jevrejeva, S. (2004). Application of the cross wavelet transform and wavelet coherence to geophysical time series. *Nonlinear Processes in Geophysics*, *11*(5/6), 561–566. https://doi.org/10.5194/npg-11-561-2004

Happell, J. D., Chanton, J. P., & Showers, W. S. (1994). The influence of methane oxidation on the stable isotopic composition of methane emitted from Florida swamp forests. *Geochimica et Cosmochimica Acta*, *58*(20), 4377–4388. https://doi.org/10.1016/0016-7037(94)90341-7

Hayashi, K., Tokida, T., Kajiura, M., Yanai, Y., & Yano, M. (2015). Cropland soil–plant systems control production and consumption of methane and nitrous oxide and their emissions to the atmosphere. *Soil Science & Plant Nutrition*, *61*(1), 2–33. https://doi.org/10.1080/00380768.2014.994469

Himmelblau, D. M. (1964). Diffusion of dissolved gases in liquids. *Chemical Reviews*, *64*(5), 527–550. https://doi.org/10.1021/cr60231a002

Hoffmann, M., Schulz-Hanke, M., Garcia Alba, J., Jurisch, N., Hagemann, U., Sachs, T., et al. (2017). A simple calculation algorithm to separate high-resolution CH_4 flux measurements into ebullition- and diffusion-derived components. *Atmospheric Measurement Techniques*, *10*(1), 109–118. https://doi.org/10.5194/amt-10-109-2017

Hosono, T., & Nouchi, I. (1998). Diurnal change in methane flux from a rice paddy related to the soil temperature. *Journal of Agricultural Meteorology*, *54*(4), 329–336. https://doi.org/10.2480/agrmet.54.329

Kato, C., Imoto, H., Nishimura, T., & Miyazaki, T. (2013). Investigation of changes in soil CO_2 concentration by using compact buried tubing soil gas monitoring system. *Japanese Society of Soil Physics*, *124*, 25–33.

Kellner, E., Baird, A. J., Oosterwoud, M., Harrison, K., & Waddington, J. M. (2006). Effect temperature and atmospheric pressure on methane (CH_4) ebullition from near-surface peats. *Geophysical Research Letters*, *33*, L18405. https://doi.org/10.1029/2006GL027509

Khalil, M. A. K., Shearer, M. J., Rasmussen, R. A., Duan, C., & Ren, L. (2008). Production, oxidation, and emissions of methane from rice fields in China. *Journal of Geophysical Research*, *113*, G00A04. https://doi.org/10.1029/2007JG000461

Komiya, S., Noborio, K., Katano, K., Pakoktom, T., Siangliw, M., & Toojinda, T. (2015). Contribution of ebullition to methane and carbon dioxide emission from water between plant rows in a tropical rice paddy field. *International Scholarly Research Notices*, *2015*, 1–8. https://doi.org/10.1155/2015/623901

Krüger, M., Eller, G., Conrad, R., & Frenzel, P. (2002). Seasonal variation in pathways of CH_4 production and in CH_4 oxidation in rice fields determined by stable carbon isotopes and specific inhibitors. *Global Change Biology*, *8*(3), 265–280. https://doi.org/10.1046/j.1365-2486.2002.00476.x

Lee, H. J., Jeong, S. E., Kim, P. J., Madsen, E. L., & Jeon, C. O. (2015). High resolution depth distribution of Bacteria, Archaea, methanotrophs, and methanogens in the bulk and rhizosphere soils of a flooded rice paddy. *Frontiers in Microbiology*, *6*(JUN), 1–13. https://doi.org/10.3389/fmicb.2015.00639

Marik, T., Fischer, H., Conen, F., & Smith, K. (2002). Seasonal variations in stable carbon and hydrogen isotope ratios in methane from rice fields. *Global Biogeochemical Cycles*, *16*(4), 1094. https://doi.org/10.1029/2001GB001428

Miyata, A., Iwata, T., Nagai, H., Yamada, T., Yoshikoshi, H., Mano, M., et al. (2005). Seasonal variation of carbon dioxide and methane fluxes at single cropping paddy fields in central and western Japan. *Phyton (B. Aires)*, *45*, 89–97.

Nakagawa, F., Yoshida, N., Sugimoto, A., Wada, E., Yoshioka, T., Ueda, S., & Vijarnsorn, P. (2002). Stable isotope and radiocarbon compositions of methane emitted from tropical rice paddies and swamps in southern Thailand. *Biogeochemistry*, *61*(1), 1–19. https://doi.org/10.1023/a:1020270032512

Nishiuchi, S., Yamauchi, T., Takahashi, H., Kotula, L., & Nakazono, M. (2012). Mechanisms for coping with submergence and waterlogging in rice. *Rice*, *5*(1), 2. https://doi.org/10.1186/1939-8433-5-2

Poindexter, C. M., Baldocchi, D. D., Matthes, J. H., Knox, S. H., & Variano, E. A. (2016). The contribution of an overlooked transport process to a wetland's methane emissions. *Geophysical Research Letters*, *43*, 6276–6284. https://doi.org/10.1002/2016GL068782

Rao, D. K., Bhattacharya, S. K., & Jani, R. A. (2008). Seasonal variations of carbon isotopic composition of methane from Indian paddy fields. *Global Biogeochemical Cycles*, *22*, GB1004. https://doi.org/10.1029/2006GB002917

Saunois, M., Bousquet, P., Poulter, B., Peregon, A., Ciais, P., Canadell, J. G., et al. (2016). The global methane budget 2000–2012. *Earth System Science Data*, *8*(2), 697–751. https://doi.org/10.5194/essd-8-697-2016

Schmidt, H., Eickhorst, T., & Tippkötter, R. (2011). Monitoring of root growth and redox conditions in paddy soil rhizotrons by redox electrodes and image analysis. *Plant and Soil*, *341*(1–2), 221–232. https://doi.org/10.1007/s11104-010-0637-2

Schütz, H., Seiler, W., & Conrad, R. (1989). Processes involved in formation and emission of methane in rice paddies. *Biogeochemistry*, *7*(1), 33–53. https://doi.org/10.1007/BF00000896

Sugimoto, A., & Wada, E. (1993). Carbon isotopic composition of bacterial methane in a soil incubation experiment: Contributions of acetate and. *Geochimica et Cosmochimica Acta*, *57*(16), 4015–4027. https://doi.org/10.1016/0016-7037(93)90350-6

Takai, Y. (1970). The mechanism of methane fermentation in flooded paddy soil. *Soil Science & Plant Nutrition*, *16*(6), 238–244. https://doi.org/10.1080/00380768.1970.10433371

Tokida, T., Cheng, W., Adachi, M., Matsunami, T., Nakamura, H., Okada, M., & Hasegawa, T. (2013). The contribution of entrapped gas bubbles to the soil methane pool and their role in methane emission from rice paddy soil in free-air [CO_2] enrichment and soil warming experiments. *Plant and Soil*, *364*(1–2), 131–143. https://doi.org/10.1007/s11104-012-1356-7

Tokida, T., Miyazaki, T., & Mizoguchi, M. (2009). Physical controls on ebullition losses of methane from peatlands. In *Northern peatlands and carbon cycling*, *Geophysical Monograph Series* (Vol. 184, pp. 219–228). Washington, DC: AGU. https://doi.org/10.1029/2008GM000805

Tokida, T., Miyazaki, T., Mizoguchi, M., Nagata, O., Takakai, F., Kagemoto, A., & Hatano, R. (2007). Falling atmospheric pressure as a trigger for methane ebullition from peatland. *Global Biogeochemical Cycles*, *21*, GB2003. https://doi.org/10.1029/2006GB002790

Tokida, T., Nakajima, Y., Hayashi, K., Usui, Y., Katayanagi, N., Kajiura, M., et al. (2014). Fully automated, high-throughput instrumentation for measuring the $\delta^{13}C$ value of methane and application of the instrumentation to rice paddy samples. *Rapid Communications in Mass Spectrometry*, *28*(21), 2315–2324. https://doi.org/10.1002/rcm.7016

Torrence, C., & Compo, G. P. (1998). A practical guide to wavelet analysis. *Bulletin of the American Meteorological Society*, *79*(1), 61–78. https://doi.org/10.1175/1520-0477(1998)079<0061:APGTWA>2.0.CO;2

Tyler, S. C., Bilek, R. S., Sass, R. L., & Fisher, F. M. (1997). Methane oxidation and pathways of production in a Texas paddy field deduced from measurements of flux, $\delta^{13}C$, and δD of CH_4. *Global Biogeochemical Cycles*, *11*(3), 323–348. https://doi.org/10.1029/97GB01624

Tyler, S. C., Brailsford, G. W., Yagi, K., Minami, K., & Cicerone, R. J. (1994). Seasonal variations in methane flux and $\delta^{13}CH_4$ values for rice paddies in Japan and their implications. *Global Biogeochemical Cycles*, *8*(1), 1–12. https://doi.org/10.1029/93GB03123

Wassmann, R., Neue, H. U., Alberto, M. C. R., Lantin, R. S., Bueno, C., Llenaresas, D., et al. (1996). Fluxes and pools of methane in wetland rice soils with varying organic inputs. *Environmental Monitoring and Assessment*, *42*(1–2), 163–173. https://doi.org/10.1007/BF00394048

Waters, I., Armstrong, W., Thompson, C. J., Setter, T. L., Adkins, S., Gibbs, J., & Greenway, H. (1989). Diurnal changes in radial oxygen loss and ethanol metabolism in roots of submerged and non-submerged rice seedlings. *The New Phytologist*, *113*(4), 439–451. https://doi.org/10.1111/j.1469-8137.1989.tb00355.x

Watt, M., & Evans, J. R. (1999). Linking development and determinacy with organic acid efflux from proteoid roots of white lupin grown with low phosphorus and ambient or elevated atmospheric CO_2 concentration. *Plant Physiology*, *120*(3), 705–716. https://doi.org/10.1104/pp.120.3.705

Whiticar, M. J., Faber, E., & Schoell, M. (1986). Biogenic methane formation in marine and freshwater environments: CO_2 reduction vs. acetate fermentation—Isotope evidence. *Geochimica et Cosmochimica Acta*, *50*(5), 693–709. https://doi.org/10.1016/0016-7037(86)90346-7

Yagi, K., Chairoj, P., Tsuruta, H., Cholitkul, W., & Minami, K. (1994). Methane emission from rice paddy fields in the central plain of Thailand. *Soil Science & Plant Nutrition*, *40*(1), 29–37. https://doi.org/10.1080/00380768.1994.10414275

Yan, X., Akiyama, H., Yagi, K., & Akimoto, H. (2009). Global estimations of the inventory and mitigation potential of methane emissions from rice cultivation conducted using the 2006 intergovernmental panel on climate change guidelines. *Global Biogeochemical Cycles*, *23*, GB2002. https://doi.org/10.1029/2008GB003299

Zhang, G., Ji, Y., Ma, J., Xu, H., Cai, Z., & Yagi, K. (2012). Intermittent irrigation changes production, oxidation, and emission of CH_4 in paddy fields determined with stable carbon isotope technique. *Soil Biology. The Biochemist*, *52*, 108–116. https://doi.org/10.1016/j.soilbio.2012.04.017

Zhang, G., Ma, J., Yang, Y., Yu, H., Shi, Y., & Xu, H. (2017). Variations of stable carbon isotopes of CH_4 emission from three typical rice fields in China. *Pedosphere*, *27*(1), 52–64. https://doi.org/10.1016/S1002-0160(15)60096-0

Zhang, G., Yu, H., Fan, X., Ma, J., & Xu, H. (2016). Carbon isotope fractionation reveals distinct process of CH_4 emission from different compartments of paddy ecosystem. *Scientific Reports*, *6*(1), 27065. https://doi.org/10.1038/srep27065

Zhang, G., Zhang, X., Ji, Y., Ma, J., Xu, H., & Cai, Z. (2011). Carbon isotopic composition, methanogenic pathway, and fraction of CH_4 oxidized in a rice field flooded year-round. *Journal of Geophysical Research*, *116*, G04025. https://doi.org/10.1029/2011JG001696

Zhang, G. B., Ji, Y., Ma, J., Liu, G., Xu, H., & Yagi, K. (2013). Pathway of CH_4 production, fraction of CH_4 oxidized, and ^{13}C isotope fractionation in a straw-incorporated rice field. *Biogeosciences*, *10*(5), 3375–3389. https://doi.org/10.5194/bg-10-3375-2013

Erratum

In the originally published version of this article, the in-text citations to the panels of Figure 4 were transposed in Section 3.3.2. In Section 4.2.3, the in-text citations to Figures 3a, 3b, and 3h did not include Figure 6.

Additionally, an incorrect version of the Supporting Information published.

The article and Supporting Information have since been corrected, and this version may be considered the authoritative version of record.